J Biol Chem. 2013 Jun 14; 288(24): 17336–17346. PMCID: PMC3682535
Published online 2013 Apr 18. doi: 10.1074/jbc.M112.433441

Formation of a Quaternary Complex of HIV-1 Reverse Transcriptase with a Nucleotide-competing Inhibitor and Its ATP Enhancer[*] [S]

Maryam Ehteshami,[‡,1] Monique Nijhuis,[§] Jean A. Bernatchez,[¶,2] Christopher J. Ablenas,[¶,2] Suzanne McCormick,[‡] Dorien de Jong,[§] Dirk Jochmans,[‖] and Matthias Götte[‡¶**,3]

From the Departments of [‡]Microbiology and Immunology,
[¶]Biochemistry, and
[**]Medicine, McGill University, Montreal, Quebec H3A 2B4, Canada,
[§]Virology, Department of Medical Microbiology, University Medical Center Utrecht, 3584 CX Utrecht, The Netherlands, and
the [‖]Rega Institute for Medical Research, University of Leuven, B-3000 Leuven, Belgium

[3] Recipient of a career award from the Fonds de la Recherche en Santé du Québec. To whom correspondence should be addressed: McGill University, Dept. of Microbiology and Immunology, Duff Medical Bldg. (D-6), 3775 University St., Montreal, Quebec H3A 2B4, Canada., Tel.: Phone: 514-398-1365; Fax: 514-398-7052; E-mail: matthias.gotte@mcgill.ca.

[1]Recipient of a Canadian Institutes of Health Research doctoral research award. Present address: Dept. of Pediatrics, Emory University/Veterans Affairs Medical Hospital, Decatur, GA 30033.

[2]Recipient of a doctoral training award from the Fonds de la Recherche en Santé du Québec and supported by the Canadian Institutes of Health Research Strategic Training Initiative in Chemical Biology.

Received 2012 Nov 2; Revised 2013 Apr 18

Abstract

Nucleotide-competing reverse transcriptase inhibitors were shown to bind reversibly to the nucleotide-binding site of the reverse transcriptase (RT) enzyme of human immunodeficiency virus type 1 (HIV-1). Here, we show that the presence of ATP can enhance the inhibitory effects of the prototype compound INDOPY-1. We employed a combination of cell-free and cell-based assays to shed light on the underlying molecular mechanism. Binding studies and site-specific footprinting experiments demonstrate the existence of a stable quaternary complex with HIV-1 RT, its nucleic acid substrate, INDOPY-1, and ATP. The complex is frozen in the post-translocational state that usually accommodates the incoming nucleotide substrate. Structure-activity relationship studies show that both the base and the phosphate moieties of ATP are elements that play important roles in enhancing the inhibitory effects of INDOPY-1. *In vitro* susceptibility measurements with mutant viruses containing amino acid substitutions K70G, V75T, L228R, and K219R in the putative ATP binding pocket revealed unexpectedly a hypersusceptible phenotype with respect to INDOPY-1. The same mutational cluster was previously shown to reduce susceptibility to the pyrophosphate analog phosphonoformic acid. However, in the absence of INDOPY-1, ATP can bind and act as a pyrophosphate donor under conditions that favor formation of the pre-translocated RT complex. We therefore conclude that the mutant enzyme facilitates simultaneous binding of INDOPY-1 and ATP to the post-translocated complex. Based on these data, we propose a model in which the bound ATP traps the inhibitor, which, in turn, compromises its dissociation.

Keywords: DNA Polymerase, Drug Action, Drug Resistance, HIV-1, Reverse Transcription

Introduction

The reverse transcriptase (RT)[4] of human immunodeficiency virus type 1 (HIV-1) is an RNA- and DNA-dependent DNA polymerase that remains a prime target for antiretroviral intervention. The two approved classes of RT inhibitors are nucleoside analog (NRTI) and non-nucleoside analog (NNRTI) RT inhibitors. Phosphorylated NRTIs compete with natural deoxynucleoside triphosphates (dNTPs), bind to the polymerase active site, and cause chain termination of the growing DNA strand. Binding of NNRTIs to a hydrophobic pocket near the polymerase active site results in inhibition of nucleotide incorporation without

directly competing with the substrate (1–5).

Indolopyridone-derived compounds (6, 7) represent a novel, investigational class of RT inhibitors that suppress DNA polymerization through a mechanism that is distinct from both NRTIs and NNRTIs. INDOPY-1 (Fig. 1), the prototype compound of this class, was shown to be active against NNRTI-resistant HIV strains (6, 7). However, certain NRTI resistance-conferring mutations in the vicinity of the polymerase active site confer resistance to this inhibitor (6, 7). Mutation M184V that confers high level resistance to the NRTI lamivudine (3TC) was shown to reduce susceptibility to INDOPY-1. This mutation discriminates against both inhibitors at the level of binding (8–11). In contrast, Y115F in HIV-1 RT appears to enhance nucleotide binding at the cost of inhibitor binding. As such, both mutations together amplify the level of resistance. These findings represent strong evidence to show that despite distinct structures, INDOPY-1 may share some common properties with NRTIs.

Different classes of RT inhibitors can bind to different conformations of the RT·nucleic acid complex. Following incorporation of the nucleotide substrate and release of the pyrophosphate (PPi) product, the RT enzyme can rapidly shuttle between pre- and post-translocational states (12–17). Footprinting studies revealed that NRTIs and natural nucleoside triphosphates (dNTPs) can only bind to and trap the RT complex in its post-translocated state (13). INDOPY-1 behaves identically in these assays (6). Conversely, the PPi analog foscarnet (phosphonoformic acid, PFA) traps the complex in the pre-translocational state (15). However, unlike NRTIs and dNTPs, INDOPY-1 does not require the templated nucleotide for base pairing. It rather seems that the compound recognizes the ultimate base pair. "Hot spots" for inhibition of DNA synthesis are seen when the primer 3′ terminus contains a pyrimidine base (6, 7). Together, these data suggest that the binding sites for INDOPY-1 and the dNTP substrate partially overlap. Hence, RT inhibitors with the aforementioned properties are collectively referred to as "nucleotide-competing RT inhibitors" (NcRTIs) (8, 18).

In this study, we demonstrate that the presence of adenosine triphosphate (ATP) can enhance the inhibitory effects of INDOPY-1. Previous studies have shown that ATP can also act as a PPi donor that promotes excision of incorporated NRTIs (19). This reaction provides an important mechanism for resistance to this class of inhibitors, in particular to zidovudine (AZT). However, in this context, ATP traps the pre-translocated RT complex (20). Here, we utilized a combination of cell-based and cell-free assays to characterize the mode of binding of ATP in conjunction with INDOPY-1. We demonstrate that ATP and INDOPY-1 can form a quaternary complex with RT and its nucleic acid substrate. These findings point to a highly flexible ATP-binding site that can accommodate this ligand in various orientations in both pre- and post-translocational conformations. We conclude that the bound ATP compromises dissociation of INDOPY-1 from a post-translocated complex.

EXPERIMENTAL PROCEDURES

Materials The heterodimeric (p66/p51) HIV-1 RT enzyme was expressed in *Escherichia coli* and purified as described previously (21). Site-directed mutagenesis was performed using the Stratagene QuikChange procedure. WT RT refers to the wild-type enzyme (HXB2 strain). TAM1 RT contains mutations M41L, D67N, L210W, and T215Y. TAM2 RT contains mutations D67N, K70R, T215F, and K219Q. "Remodeled TAMs" RT harbors mutations K70G, V75T, L228R, and K219R. Oligonucleotides were chemically synthesized and purchased from IDT with the exception of RNA template PBS-250 that was synthesized through *in vitro* transcription with T7 RNA polymerase (22). The DNA primer was either synthesized with a fluorescent Cy5 or Alexa488 label at its 5′-end or ^{32}P-radiolabeled with [γ-^{32}]ATP and T4 polynucleotide kinase (Fermentas) (13). Alexa555 quencher dUTP was purchased from Invitrogen. The RT inhibitor INDOPY-1 was obtained through the AIDS Research and Reference Reagent Program (Division of AIDS NIAID, National Institutes of Health), and Tibotec BVBA is the reagent contributor. Natural and modified nucleotides were purchased from Fermentas and TriLink, respectively (chemical structures are provided in supplemental Fig. 1).

Single Nucleotide Incorporation Assay A 3-fold excess of DNA template (C1-A, 5′-GTAACTAGAGATCCCTCAGACCCTTTTAGTCAGAAT) was hybridized to 50 nM of a fluorescently labeled DNA primer (8aT_Cy5, 5′-Cy5-TTCTGACTAAAAGGGTCTGAGGGAT). DNA·RNA hybrids

were formed in a buffer containing 50 mM Tris-HCl, pH 7.8, and 50 mM NaCl. Samples were heated to 95 °C for 3 min followed by a gradual decrease to room temperature. The hybrid was then incubated with 50 nM HIV-1 RT in a buffer containing 50 mM Tris-HCl, pH 7.8, 50 mM NaCl, as well as varying amounts of ATP and increasing concentrations of INDOPY-1 (0–18 μM). Nucleotide incorporation was initiated with the addition of 6 mM $MgCl_2$ and 100 nM dCTP at 37 °C and was allowed to proceed for 5 min. Samples were resolved on a 12% denaturing polyacrylamide gel and analyzed with a phosphorimager instrument (Amersham Biosciences) using Quantity One and ImageQuant software.

Multisite Incorporation Assay on a Heteropolymeric Template A 2-fold molar excess of PBS-250 RNA template was hybridized to 50 nM of 5′-radiolabeled PBS-28 DNA primer (5′-CTTTCAGGTCCCTGTTCGGGCGCCACTG). The hybrid was then incubated with 125 nM RT in a buffer containing 50 mM Tris-HCl, pH 7.8, 50 mM NaCl, and 10 μM of each dATP, dTTP, dGTP, and dCTP. DNA synthesis was initiated by the addition of 6 mM $MgCl_2$ in the absence or presence of inhibitor and NTPs at 37 °C. DNA synthesis was stopped at defined time points by the addition of formamide loading dye. Samples were subsequently resolved on a 12% denaturing polyacrylamide gel. Similar conditions were employed for monitoring AZT-MP excision whereby 50 nM DNA primer·template were incubated with 250 nM RT and 10 μM AZP-TP in the presence of 0.5 μM dNTPs and 3.5 mM pyrophosphatase-treated ATP. Reactions were preincubated at 37 °C for 5 min and then initiated with 6 mM $MgCl_2$. AZT-MP excision and DNA synthesis rescue was measured at various time points up to 90 min. DNA synthesis was visualized on 12% denaturing polyacrylamide gels.

Band Shift Experiments 50 nM DNA·DNA hybrid (primer, PPT-24Cy5 5′-Cy5-ACTTTTTAAAAGAAAAGGGGGGAT; template, PPT-57 5′-CGTTGGGAGTGAATTAGCCCTTCCAGTCCCCCCTTTTCTTTTAAAAAGTGGCTAAGA) was incubated with 5-fold molar excess of WT RT enzyme in the presence of 50 mM Tris-HCl, pH 7.8, 50 mM NaCl, and increasing concentrations of INDOPY-1 (0–4 μM). The stability of enzyme binding to the nucleic acid substrate was assessed in the absence or presence of ATP by the addition of 1.5 μg/μl heparin trap. Samples were incubated for 15 min at 37 °C and visualized on a nondenaturing 6% polyacrylamide gel.

In Vitro IC_{50} Assay 40 nM of the DNA template containing an Alexa-488 fluorescent dye at the 5′ terminus (5′-Alexa488-AGTCCCCCCTTTTCTTTTAAAAAGTGGCTAAGA) was hybridized to a 3-fold molar excess of DNA primer (5′-TTAAAAGAAAAGGGGGG). The hybrid was then incubated with 1 nM RT in a buffer containing 50 mM Tris-HCl, pH 7.8, 80 mM KCl, 0.025% CHAPS, 6 mM $MgCl_2$, 0.1 mM EGTA, and 1 mM DTT. 200 nM of nucleotide mix containing dATP, dCTP, dGTP, and a modified dUTP were added along with INDOPY-1 (0–30 μM). The modified dUTP contains an Alexa555 quencher, which upon incorporation quenches excitation by Alexa488 present on the DNA template (23). The signal was monitored over a period of 60 min using SPECTRAmax M5 fluorometer where reductions in Alexa488 emission signals are indicative of increased DNA polymerization.

Site-specific Footprinting Translocation of the enzyme relative to the nucleic acid substrate was monitored using Fe^{2+} site-specific footprinting techniques as described previously (13, 24). Briefly, 150 nM of primer (PPT-20 5′-TTAAAAGAAAAGGGGGGACT) was hybridized to 50 nM DNA template PPT-57 (5′-CGTTGGGAGTGAATTAGCCCTTCCAGTCCCCCCTTTTCTTTTAAAAGTGGCTAAGA) containing a radiolabel at the 5′ terminus. The DNA hybrid was then incubated with 750 nM RT (WT or mutant) in a buffer containing 120 mM sodium cacodylate, pH 7, 20 mM NaCl, and 10 mM $MgCl_2$ with and without 1 mM ATP as indicated. The samples were then incubated with a concentration gradient of INDOPY-1 and treated with Fe^{2+} after a 10-min incubation at 37 °C. Samples were resolved on a 12% denaturing polyacrylamide gel.

Standard deviations for all datasets were calculated through GraphPad Prism software. Briefly, the sum of the square of the difference between each value and the mean was divided by $n - 1$. The square root of this value represents the standard deviation as calculated by the software.

In Silico Docking of INDOPY-1 and ATP Binding models were generated using the crystal structure of the HIV-1 RT/chain-terminated primer·template·dTTP ternary complex (PDB code 1RTD) (25). The dTTP substrate present at the active site of the 1RTD structure was removed prior to INDOPY-1 docking. ATP

was subsequently docked to the structural model with INDOPY-1 present in the active site. The structure of INDOPY-1 was constructed in ChemDraw (CambridgeSoft Corp.), energy-minimized for 100 cycles under default parameters using Chimera, and saved as a PDB file. The structures of the protein and the small molecule were prepared for docking using AutoDockTools 1.5.4. Subsequently, the docking was performed using AutoDock Vina. Modeling of ATP binding in the context of INDOPY-1 was performed using the same protein crystal structure as above; however, the coordinates for the best candidate pose for INDOPY-1 binding were this time introduced into the PDB file of the protein. Molecular graphics images were produced using the UCSF Chimera package from the Resource for Biocomputing, Visualization, and Informatics at the University of California, San Francisco (supported by National Institutes of Health Grant P41 RR-01081).

Generation of Recombinant Viruses The N terminus of RT (amino acids 25–314) of HIV-1 clones containing the TAM1, TAM2, and remodeled TAM mutations (26) were amplified, digested, and ligated using the previously described NRT-vector system (27). Clones were verified by sequence analysis. To generate recombinant viruses, RT molecular clones were transfected in 293T cells. For this, 5–6 × 10^6 293 T cells were seeded the day prior to transfection to achieve 90–95% confluence on the day of transfection. For transfection, 10 μg of plasmid DNA and Lipofectamine 2000 (Invitrogen) were used according to the manufacturer's protocol. Two days after transfection, recombinant virus was harvested. 50% tissue culture infective dose was determined by end point dilution in MT2 cells or human donor peripheral blood mononuclear cells (PBMCs).

Phenotypic Drug Susceptibility Drug susceptibility was determined by a multiple cycle cell-killing assay (28). MT-2 cells (5 × 10^4 in 200 μl of RPMI 1640 medium and 10% FBS per well) were plated in 96-well microplates. Recombinant virus and reference virus were inoculated for 5 days on a single 96-well plate in the presence of drug dilutions. All viruses were inoculated at multiple multiplicities of infection to adjust for any differences in viral replication capacity (RC). Fold change values were calculated by dividing the mean 50% effective concentration for a recombinant virus by that of the HXB2 reference strain. Fold changes are averages of at least two separate experiments. Drug susceptibility was also analyzed in donor PBMCs. Here, activated PBMCs were infected with a recombinant virus or reference strain using a multiplicity of infection of 0.001 (PBMC titration) incubated for 2 h at 37 °C, after which cells were washed twice. Subsequently, 0.2 × 10^6 cells/well were plated into a 96-well plate with increasing drug concentrations. p24 was analyzed on days 0 and 7.

RESULTS

ATP Enhances INDOPY-1-mediated Inhibition of DNA Synthesis We monitored single nucleotide incorporations with purified HIV-1 RT in the presence of increasing concentrations of INDOPY-1. This assay revealed an IC_{50} value of ~2.5 μM in the absence of ATP (Fig. 2*A*). In the presence of physiologically relevant concentrations of 3 mM ATP (29), we determined an IC_{50} value of ~0.25 μM. IC_{50} values for INDOPY-1 are shown as a function of increasing concentrations of ATP, which demonstrates a dose-dependent effect of the enhancer molecule.

We next asked whether the enhancement of inhibition was specific to the nucleotide base of ATP. To address this issue, we monitored multiple nucleotide incorporations on a heteropolymeric template. In the absence of inhibitor, the full-length DNA product appeared within 7 min (Fig. 2*B*). Saturating concentrations of 6 μM INDOPY-1 reduced the amount of DNA product observed over the same period of time. When DNA synthesis was compared in the presence of INDOPY-1 and 3 mM ATP, UTP, GTP, or CTP, we found that ATP showed the strongest enhancement of inhibition. GTP showed subtle but visible increases in inhibition, whereas pyrimidines UTP and CTP do not seem to act as enhancers. In the absence of INDOPY-1, the presence of NTPs showed only subtle effects on DNA synthesis (data not shown). These findings suggest that the base moiety represents an important structural element in enhancing the inhibitory effects of NcRTIs.

Structure-Activity Relationship Studies for ATP Enhancement We monitored inhibition of DNA synthesis and its enhancement in the presence of derivatives of ATP with modifications in base, sugar, and phosphate moieties, respectively (for structural details, see supplemental Fig. 1). The loss of the 6-amino group of the

purine (benzimidazole and 2-aminopurine), as well as modifications at this position (*N*6-methyl) severely compromised the enhancement of inhibition (Fig. 3*A*). Note that in contrast to 2-aminopurine, the related GTP and 2-amino-ATP retain their ability to increase inhibition (Figs. 2*B* and 3*B*). Hence, it appears that the presence of a hydrogen bond donor or acceptor is essential at position 6. Modifications at the smaller ring did not show any significant effect (Fig. 3*B*). In the absence of INDOPY-1, each of these compounds had no significant effect on polymerization under the same conditions (data not shown).

We also studied several ATP derivatives with modifications primarily at the 2′- and/or 3′-position of the sugar ring. Neither of these compounds showed any significant reductions in enhancement of inhibition. Modifications at the phosphate moiety show a stronger effect. Whereas 1-thio-ATP retains the ability to enhance the inhibitory effect of INDOPY-1, marked decreases are seen in the following order: ATP > ADP > AMP > A (Fig. 3*B*). Taken together, an intact triphosphate moiety together with a hydrogen bond donor or acceptor at position 6 of the purine base seem to be important structural elements that facilitate binding of the ATP enhancer.

ATP and INDOPY-1 Form a Quaternary Complex with RT and Its Nucleic Acid Substrate The effect of ATP on INDOPY-1-mediated inhibition of DNA synthesis suggest the formation of a quaternary complex. We employed band shift experiments to test this hypothesis. In this assay, INDOPY-1 can bind to and stabilize the RT·DNA·DNA complex (Fig. 4*A*) (6, 8). The resulting ternary complex is resistant to the challenge with heparin that traps the dissociated enzymes. Increasing concentrations of INDOPY-1 correlate with an increased stability of the complex (Fig. 4*A*). In the absence of INDOPY-1, ATP alone has no effect on complex stabilization. In the presence of ATP, stable complex formation is observed at lower concentrations of INDOPY-1. The $K_{d(app)}$ value for INDOPY-1 is 216.5 nM (±56.2). In the presence of ATP, this value is decreased to 15.4 nM (±1.8) (Fig. 4*B*). Thus, the enhancing effect of ATP on INDOPY-1-mediated inhibition of RT correlates with the formation of a stable quaternary complex.

Binding Modes of ATP ATP is able to act as a PPi donor that removes incorporated NRTIs from the 3′-end of the primer. Like PFA, ATP binds to and exerts this function through the pre-translocational complex (13, 16, 17, 19, 20, 30–33). However, INDOPY-1 was shown to trap the post-translocated complex (6). To address this apparent disconnect, we examined the potency of INDOPY-1 in the context of a series of RT mutations that are known to affect binding of ATP. Mutations that confer resistance to the NRTI AZT, referred to as thymidine-associated mutations (TAM1 or TAM2), facilitate binding of ATP in an orientation that promotes excision (19, 20, 31, 34, 35). We therefore determined EC_{50} values for INDOPY-1, in MT-2 cells in the presence of HIV-1 virus containing either TAM1 (M41L, D67N, L210W, and T215Y) or TAM2 (D67N, K70R, T215F, and K219Q) mutational clusters (Table 1). TAM1 does not affect susceptibility to INDOPY-1, whereas TAM2 appears to confer low levels of resistance to the inhibitor (Table 1). We have also tested a mutational cluster, referred to as remodeled TAMs (K70G, V75T, L228R, and K219R) (36). This pattern emerges in NRTI experienced patients who are infected with TAM-containing HIV variants prior to PFA salvage therapy. Remodeled TAMs were shown to reduce resistance to AZT and confer resistance to PFA. Here, we confirmed this phenotype in biochemical assays. Whereas TAM1 and TAM2 show subtle increases in sensitivity to PFA, the RT enzyme containing remodeled TAMs is only inhibited at markedly higher concentrations of PFA (Fig. 5). This effect is in part mediated through K70G, which is in agreement with previous reports that analyzed K70G in a different mutational context (37, 38). Moreover, DNA synthesis in the presence of AZT-TP and the PPi donor ATP showed reduced excision of the incorporated chain terminator when remodeled TAM was compared with TAM1- or TAM2-containing RT enzymes (Fig. 6). Hence, remodeled TAMs may directly affect the binding site of ATP, although several other mutations also confer resistance to PFA (39–42). As a control, we also measured susceptibility to these compounds in cell culture, and in agreement with Mathiesen *et al.* (36), remodeled TAMs conferred resistance to PFA, whereas decreased susceptibility to AZT was only observed with strains harboring TAM1 and TAM2 (Table 1). Remodeled TAMs cause hypersusceptibility to INDOPY-1 (0.2-fold change in EC_{50} when compared with WT HIV-1). The presence of remodeled TAMs in the purified RT also caused a decrease in IC_{50} values for INDOPY-1, which is in agreement with the cell culture data (Table 2). This effect is more pronounced in the presence of ATP, suggesting that this mutational cluster can promote binding of INDOPY-1 and ATP, respectively (Table 2).

An improved binding of INDOPY-1 and ATP against a backbone of remodeled TAMs is difficult to reconcile with the findings that these mutations diminish resistance to AZT (36). However, the excision-competent complex with ATP exists in the pre-translocated conformation, whereas INDOPY-1 traps the post-translocated complex. To establish that the quaternary complex with INDOPY-1 and ATP remains in the post-translocated conformation, we performed site-specific footprinting experiments that allow us to distinguish between both pre- and post-translocational states (Fig. 7*A*) (13, 15). As the concentration of INDOPY-1 increases, the cleavage pattern with WT RT is shifting from pre- to post-translocation, as described previously (6). Here, the data further show that the presence of ATP lowers the concentration of INDOPY-1 required to cause a complete shift toward post-translocation (Fig. 7). These findings demonstrate that ATP indeed stabilizes the complex with INDOPY-1 in the post-translocated conformation. The effect of INDOPY-1 on the translocational state is slightly increased against a backbone of remodeled TAMs (Fig. 7, *A* and *B*), which is in agreement with the hypersusceptible phenotype.

Together, these data suggest that remodeled TAMs confer a post-translocational bias that reduces PFA susceptibility and ATP-dependent excision of AZT-MP, both of which occur in the pre-translocated state. At the same time, the increased access to the post-translocated complex results in INDOPY-1 hypersusceptibility.

DISCUSSION

NcRTIs, like the prototype compound INDOPY-1, represent a novel class of small molecules that inhibit HIV-1 RT at concentrations in the submicromolar range. Enzyme kinetics and *in vitro* selection experiments provided strong evidence to show that the binding site of INDOPY-1 overlaps with the nucleotide-binding site (6, 8). Site-specific footprinting experiments further revealed that the inhibitor, like the natural dNTP substrate, traps the RT complex in its post-translocational state (6). Here, we show that the presence of ATP can significantly enhance the inhibitory effect of INDOPY-1. We studied the underlying molecular mechanism with particular focus on the binding mode and orientation of the ATP enhancer molecule.

A limited structure-activity relationship analysis revealed that the phosphate and base moieties of ATP are required to promote this effect. The enhancement of inhibition decreases in the following order: ATP > ADP > AMP. Pyrimidines UTP and CTP are inactive, whereas purines ATP and, to a lesser extent, GTP are active enhancer molecules. In attempts to provide a better understanding of these findings, we also included several ATP derivatives in this analysis. The data suggest that the presence of a hydrogen bond donor or acceptor at position 6 of the purine ring system is crucial for enhancing NcRTI-mediated inhibition. The specificity for purine analogs also points to a unique feature of the ATP-binding site that is distinct from the dNTP-binding site, which needs to accommodate both purines and pyrimidines. These results are not unexpected, given that ribonucleotides bind to this site with low affinity due to a steric conflict between the 2′-OH group and residue Tyr-115 in HIV-1 RT (43, 44). Moreover, INDOPY-1 competes with dNTP substrates, which suggests that the nucleotide-binding site is at least in part occupied by the inhibitor.

Like the natural dNTP substrate, INDOPY-1 can form a stable complex with HIV-1 RT and its primer·template substrate (6, 8, 45). These complexes are resistant to challenges with an enzyme trap, such as heparin. Crystal structures of HIV-1 RT with and without a bound dNTP substrate have shown that the fingers subdomain close down and trap the incoming dNTP, which stabilizes the complex (25, 46). A similar scenario has been postulated for the ternary complex with INDOPY-1 (6, 8), although the particular conformation of the “closed” structure likely differs from the ternary RT·DNA·DNA·dNTP complex. Here, we show that concentrations of ATP in the low millimolar range can reduce the amount of INDOPY-1 required to stabilize the RT complex. Together, these data provide strong evidence to suggest that RT, its nucleic acid substrate, the inhibitor, and the ATP enhancer molecule form a stable quaternary complex.

Binding of ATP to HIV-1 RT has previously been demonstrated in a different context (19, 20, 35). ATP can bind in an orientation that facilitates the excision of the ultimate nucleotide from the primer terminus. This reaction provides an important mechanism for resistance to NRTIs. TAM1 or TAM2 mutational clusters were shown to increase rates of excision of incorporated AZT-MP, and other inhibitors of this class (19). Structures that contain the dinucleotide tetraphosphate product suggest that the resistance-conferring mutations can affect the orientation of the base moiety of the bound ATP thereby facilitating binding and its

function as a PPi donor (20). Site-specific footprinting and crystal structures of a related polymerase have shown that the PPi analog PFA stabilizes the pre-translocational conformation though closure of the fingers subdomain (15, 47). By contrast, INDOPY-1 traps the post-translocational state, which raised the question whether ATP can bind to both translocational states of the RT complex. Our footprinting experiments provide strong support for the notion that the quaternary complex with INDOPY-1 and ATP is indeed stabilized in the post-translocational state.

To provide a more detailed picture of the ATP binding mode and orientation, we conducted *in vitro* susceptibility measurements with TAM1 (M41L, D67N, L210W, and T215Y) and TAM2 (D67N, K70R, T215F, and K219Q) and the remodeled TAMs cluster that contains mutations K70G, V75T, L228R, and K219R. Given that TAM1 and TAM2 confer resistance to AZT and facilitate ATP binding, one would expect increases in susceptibility to INDOPY-1. However, TAM1 does not appear to show any significant effect, and TAM2 shows subtle decreases in INDOPY-1 susceptibility. Conversely, given that remodeled TAMs reduce resistance to AZT and increase resistance to PFA (36), one would expect decreases in susceptibility to INDOPY-1. However, in this case we observed a hypersusceptible phenotype, and biochemical studies show that the mutations increase the effects of both INDOPY-1 and ATP. A possible explanation is that remodeled TAMs can shift the translocational equilibrium toward post-translocation, which facilitates binding of INDOPY-1. Binding of ATP and PFA to the pre-translocated conformation is at the same time reduced under these circumstances. Essentially, the diminished excision of AZT by remodeled TAMs indicates that binding of ATP to the pre-translocated complex is compromised. This effect passively promotes binding of ATP instead to the post-translocated state of the enzyme to stabilize a quaternary complex with INDOPY. This model helps to reconcile the apparent contradiction of ATP-mediated enhancement of INDOPY-1 for remodeled TAMs and diminished resistance to AZT for the same enzyme. In this context it is also important to note that TAM enzymes show the opposite effect on the translocational equilibrium and confer a pre-translocational bias (48).

Model for INDOPY-1 and ATP Binding to the Polymerase Active Site of HIV-1 RT We employed *in silico* approaches in attempts to identify possible binding pockets for INDOPY-1 and its ATP enhancer. We docked a flexible structure of INDOPY-1 to the RT crystal structure whereby the crystallized dTTP substrate was removed (Fig. 8). To validate our docking strategy, we redocked dTTP back into the polymerase active site and confirmed a high degree of similarity with the original crystal structure. In our model, INDOPY-1 binds to the nucleotide-binding site of a post-translocated complex. An important feature of this model is that the benzene ring of the inhibitor can stack with the ultimate base of the primer (Fig. 8 *A*). Binding of INDOPY-1 is severely compromised with an abasic residue at the primer terminus (data not shown), which is consistent with this model. The nitro group of the benzene ring is positioned within close proximity to residues Met-184 and Tyr-115, and changes at these positions are associated with resistance to this compound (Fig. 8*B*). Finally, the methyl group present on the pyrrole ring appears to protrude into the "unoccupied pocket" that exists between the fingers and the thumb subdomains of HIV-1 RT (Fig. 8, *C* and *D*).

We next docked ATP to the model of the ternary RT·DNA·DNA·INDOPY-1 complex (Fig. 8, *C–E*). ATP appears to bind in an orientation that is similar to the excision complex (20), although the two complexes exist in post- and pre-translocational states, respectively. The phosphate moiety of ATP interacts with the same residues as seen with the crystal structure of ATP bound to RT (20), although the base of ATP bends toward the thumb subdomain of RT and the sugar backbone of the DNA·DNA substrate. Consistent with our structure-activity relationship data, the amino group at position 6 of ATP makes possible contacts with other residues in the quaternary complex (Fig. 8, *C–E*). Finally, amino acid residues that are mutated as part of remodeled TAMs are in close proximity to the phosphate and base moiety of the docked ATP (Fig. 8*E*). In summary, according to this model, ATP can bind to the post-translocational state with INDOPY-1 bound at the active site (Fig. 8, *C–E*). It is possible that both ligands ATP and INDOPY-1 stabilize the closed complex more effectively. However, it should be noted that this docking model does not reflect the intrinsic flexibility of the fingers and thumb subdomains. As such, crystallographic data are warranted to delineate subtle differences in subdomain movements in the context of INDOPY-1/ATP *versus* dNTP binding.

Overall, the results of this study point to a highly flexible ATP-binding site of HIV-1 RT. Although previous

studies have described and characterized binding of ATP to the pre-translocated complex as a PPi donor, this work describes its binding to the post-translocated complex as an enhancer of the inhibitory effects of INDOPY-1. Together, the data identify a new binding pocket for small molecule inhibitors that can be exploited in drug discovery and development efforts to improve the properties of NcRTIs.

Acknowledgment

Anick Auger is acknowledged for excellent technical assistance.

*This work was supported in part by the Canadian Institutes of Health Research, Tibotec, and Netherlands Organisation for Scientific Research VIDI Grant 91796349.

S This article contains supplemental Fig. 1.

[4]The abbreviations used are:

RT reverse transcriptase
NcRTI nucleotide-competing RT inhibitor
PFA phosphonoformic acid
PBMC peripheral blood mononuclear cell
PPi pyrophosphate
AZT zidovudine
AZT-MP AZT-monophosphate
AZT-TP AZT-triphosphate
PDB Protein Data Bank
NRTI nucleoside analog RT inhibitor
NNRTI non-nucleoside RT inhibitor
dNTP deoxynucleotide triphosphate
NTP ribonucleotide triphosphate.

REFERENCES

1. Basavapathruni A., Anderson K. S. (2007) Reverse transcription of the HIV-1 pandemic. FASEB J. 21, 3795–3808 [PubMed: 17639073]

2. Götte M. (2004) Inhibition of HIV-1 reverse transcription: basic principles of drug action and resistance. Expert Rev. Anti-infect Ther. 2, 707–716 [PubMed: 15482234]

3. Menéndez-Arias L. (2008) Mechanisms of resistance to nucleoside analogue inhibitors of HIV-1 reverse transcriptase. Virus Res. 134, 124–146 [PubMed: 18272247]

4. Sarafianos S. G., Marchand B., Das K., Himmel D. M., Parniak M. A., Hughes S. H., Arnold E. (2009) Structure and function of HIV-1 reverse transcriptase: molecular mechanisms of polymerization and inhibition. J. Mol. Biol. 385, 693–713 [PMCID: PMC2881421] [PubMed: 19022262]

5. Sluis-Cremer N., Tachedjian G. (2008) Mechanisms of inhibition of HIV replication by non-nucleoside reverse transcriptase inhibitors. Virus Res. 134, 147–156 [PMCID: PMC2745993] [PubMed: 18372072]

6. Jochmans D., Deval J., Kesteleyn B., Van Marck H., Bettens E., De Baere I., Dehertogh P., Ivens T., Van Ginderen M., Van Schoubroeck B., Ehteshami M., Wigerinck P., Götte M., Hertogs K. (2006) Indolopyridones inhibit human immunodeficiency virus reverse transcriptase with a novel mechanism of action. J. Virol. 80, 12283–12292 [PMCID: PMC1676280] [PubMed: 17020946]

7. Zhang Z., Walker M., Xu W., Shim J. H., Girardet J. L., Hamatake R. K., Hong Z. (2006) Novel nonnucleoside inhibitors that select nucleoside inhibitor resistance mutations in human immunodeficiency virus type 1 reverse transcriptase. Antimicrob. Agents Chemother. 50, 2772–2781 [PMCID: PMC1538665] [PubMed: 16870771]

8. Ehteshami M., Scarth B. J., Tchesnokov E. P., Dash C., Le Grice S. F., Hallenberger S., Jochmans D., Götte M. (2008) Mutations M184V and Y115F in HIV-1 reverse transcriptase discriminate against "nucleotide-competing reverse transcriptase inhibitors." J. Biol. Chem. 283, 29904–29911

[PMCID: PMC2573056] [PubMed: 18728003]

9. Feng J. Y., Anderson K. S. (1999) Mechanistic studies examining the efficiency and fidelity of DNA synthesis by the 3TC-resistant mutant (184V) of HIV-1 reverse transcriptase. Biochemistry 38, 9440–9448 [PubMed: 10413520]

10. Tisdale M., Kemp S. D., Parry N. R., Larder B. A. (1993) Rapid *in vitro* selection of human immunodeficiency virus type 1 resistant to 3′-thiacytidine inhibitors due to a mutation in the YMDD region of reverse transcriptase. Proc. Natl. Acad. Sci. U.S.A. 90, 5653–5656 [PMCID: PMC46779] [PubMed: 7685907]

11. Wainberg M. A., Hsu M., Gu Z., Borkow G., Parniak M. A. (1996) Effectiveness of 3TC in HIV clinical trials may be due in part to the M184V substitution in 3TC-resistant HIV-1 reverse transcriptase. AIDS 10, S3–S10 [PubMed: 9030390]

12. Götte M. (2006) Effects of nucleotides and nucleotide analogue inhibitors of HIV-1 reverse transcriptase in a ratchet model of polymerase translocation. Curr. Pharm. Des. 12, 1867–1877 [PubMed: 16724953]

13. Marchand B., Götte M. (2003) Site-specific footprinting reveals differences in the translocation status of HIV-1 reverse transcriptase. Implications for polymerase translocation and drug resistance. J. Biol. Chem. 278, 35362–35372 [PubMed: 12819205]

14. Marchand B., Götte M. (2004) Impact of the translocational equilibrium of HIV-1 reverse transcriptase on the efficiency of mismatch extensions and the excision of mispaired nucleotides. Int. J. Biochem. Cell Biol. 36, 1823–1835 [PubMed: 15183347]

15. Marchand B., Tchesnokov E. P., Götte M. (2007) The pyrophosphate analogue foscarnet traps the pre-translocational state of HIV-1 reverse transcriptase in a Brownian ratchet model of polymerase translocation. J. Biol. Chem. 282, 3337–3346 [PubMed: 17145704]

16. Marchand B., White K. L., Ly J. K., Margot N. A., Wang R., McDermott M., Miller M. D., Götte M. (2007) Effects of the translocation status of human immunodeficiency virus type 1 reverse transcriptase on the efficiency of excision of tenofovir. Antimicrob. Agents Chemother. 51, 2911–2919 [PMCID: PMC1932533] [PubMed: 17517852]

17. Sarafianos S. G., Clark A. D., Jr., Tuske S., Squire C. J., Das K., Sheng D., Ilankumaran P., Ramesha A. R., Kroth H., Sayer J. M., Jerina D. M., Boyer P. L., Hughes S. H., Arnold E. (2003) Trapping HIV-1 reverse transcriptase before and after translocation on DNA. J. Biol. Chem. 278, 16280–16288 [PubMed: 12554739]

18. Jochmans D. (2008) Novel HIV-1 reverse transcriptase inhibitors. Virus Res. 134, 171–185 [PubMed: 18308412]

19. Meyer P. R., Matsuura S. E., Mian A. M., So A. G., Scott W. A. (1999) A mechanism of AZT resistance: an increase in nucleotide-dependent primer unblocking by mutant HIV-1 reverse transcriptase. Mol. Cell 4, 35–43 [PubMed: 10445025]

20. Tu X., Das K., Han Q., Bauman J. D., Clark A. D., Jr., Hou X., Frenkel Y. V., Gaffney B. L., Jones R. A., Boyer P. L., Hughes S. H., Sarafianos S. G., Arnold E. (2010) Structural basis of HIV-1 resistance to AZT by excision. Nat. Struct. Mol. Biol. 17, 1202–1209 [PMCID: PMC2987654] [PubMed: 20852643]

21. Le Grice S. F., Grüninger-Leitch F. (1990) Rapid purification of homodimer and heterodimer HIV-1 reverse transcriptase by metal chelate affinity chromatography. Eur. J. Biochem. 187, 307–314 [PubMed: 1688798]

22. Arts E. J., Li X., Gu Z., Kleiman L., Parniak M. A., Wainberg M. A. (1994) Comparison of deoxyoligonucleotide and tRNA(Lys-3) as primers in an endogenous human immunodeficiency virus-1 *in vitro* reverse transcription/template-switching reaction. J. Biol. Chem. 269, 14672–14680 [PubMed: 7514178]

23. Cauchon E., Falgueyret J. P., Auger A., Melnyk R. A. (2011) A high throughput continuous assay for screening and characterization of inhibitors of HIV reverse-transcriptase DNA polymerase activity. J. Biomol. Screen. 16, 518–524 [PubMed: 21474837]

24. Götte M., Maier G., Onori A. M., Cellai L., Wainberg M. A., Heumann H. (1999) Temporal coordination between initiation of HIV (+)-strand DNA synthesis and primer removal. J. Biol. Chem. 274, 11159–11169 [PubMed: 10196201]

25. Huang H., Chopra R., Verdine G. L., Harrison S. C. (1998) Structure of a covalently trapped catalytic complex of HIV-1 reverse transcriptase: implications for drug resistance. Science 282, 1669–1675 [PubMed: 9831551]

26. Ehteshami M., Götte M. (2008) Effects of mutations in the connection and RNase H domains of HIV-1 reverse transcriptase on drug susceptibility. AIDS Rev. 10, 224–235 [PubMed: 19092978]

27. van Maarseveen N. M., Huigen M. C., de Jong D, Smits AM, Boucher CA, Nijhuis M. (2006) A novel real time PCR assay to determine relative replication capacity for HIV-1 protease variants and/or reverse transcriptase variants. J. Virol. Methods 133, 185–194 [PubMed: 16368153]

28. Boucher C. A., Keulen W., van Bommel T., Nijhuis M., de Jong D., de Jong M. D., Schipper P., Back N. K. (1996) Human immunodeficiency virus type 1 drug susceptibility determination by using recombinant viruses generated from patient sera tested in a cell-killing assay. Antimicrob. Agents Chemother. 40, 2404–2409 [PMCID: PMC163542] [PubMed: 8891152]

29. Smith A. J., Meyer P. R., Asthana D., Ashman M. R., Scott W. A. (2005) Intracellular substrates for the primer-unblocking reaction by human immunodeficiency virus type 1 reverse transcriptase: detection and quantitation in extracts from quiescent- and activated-lymphocyte subpopulations. Antimicrob. Agents Chemother. 49, 1761–1769 [PMCID: PMC1087649] [PubMed: 15855493]

30. Meyer P. R., Matsuura S. E., Tolun A. A., Pfeifer I., So A. G., Mellors J. W., Scott W. A. (2002) Effects of specific zidovudine resistance mutations and substrate structure on nucleotide-dependent primer unblocking by human immunodeficiency virus type 1 reverse transcriptase. Antimicrob. Agents Chemother. 46, 1540–1545 [PMCID: PMC127181] [PubMed: 11959594]

31. Ray A. S., Murakami E., Basavapathruni A., Vaccaro J. A., Ulrich D., Chu C. K., Schinazi R. F., Anderson K. S. (2003) Probing the molecular mechanisms of AZT drug resistance mediated by HIV-1 reverse transcriptase using a transient kinetic analysis. Biochemistry 42, 8831–8841 [PubMed: 12873144]

32. Sarafianos S. G., Clark A. D., Jr., Das K., Tuske S., Birktoft J. J., Ilankumaran P., Ramesha A. R., Sayer J. M., Jerina D. M., Boyer P. L., Hughes S. H., Arnold E. (2002) Structures of HIV-1 reverse transcriptase with pre- and post-translocation AZTMP-terminated DNA. EMBO J. 21, 6614–6624 [PMCID: PMC136941] [PubMed: 12456667]

33. Boyer P. L., Sarafianos S. G., Arnold E., Hughes S. H. (2001) Selective excision of AZTMP by drug-resistant human immunodeficiency virus reverse transcriptase. J. Virol. 75, 4832–4842 [PMCID: PMC114238] [PubMed: 11312355]

34. Goldschmidt V., Marquet R. (2004) Primer unblocking by HIV-1 reverse transcriptase and resistance to nucleoside RT inhibitors (NRTIs). Int. J. Biochem. Cell Biol. 36, 1687–1705 [PubMed: 15183338]

35. Meyer P. R., Matsuura S. E., So A. G., Scott W. A. (1998) Unblocking of chain-terminated primer by HIV-1 reverse transcriptase through a nucleotide-dependent mechanism. Proc. Natl. Acad. Sci. U.S.A. 95, 13471–13476 [PMCID: PMC24843] [PubMed: 9811824]

36. Mathiesen S., Dam E., Roge B., Joergensen L. B., Laursen A. L., Gerstoft J., Clavel F. (2007) Long-term foscarnet therapy remodels thymidine analogue mutations and alters resistance to zidovudine and lamivudine in HIV-1. Antivir. Ther. 12, 335–343 [PubMed: 17591023]

37. Kisic M., Matamoros T., Nevot M., Mendieta J., Martinez-Picado J., Martínez M. A., Menéndez-Arias L. (2011) Thymidine analogue excision and discrimination modulated by mutational complexes, including

single amino acid deletions of Asp-67 or Thr-69 in HIV-1 reverse transcriptase. J. Biol. Chem. 286, 20615–20624 [PMCID: PMC3121480] [PubMed: 21504903]

38. Bradshaw D., Malik S., Booth C., Van Houtte M., Pattery T., Waters A., Ainsworth J., Geretti A. M. (2007) Novel drug resistance pattern associated with the mutations K70G and M184V in human immunodeficiency virus type 1 reverse transcriptase. Antimicrob. Agents Chemother. 51, 4489–4491 [PMCID: PMC2167988] [PubMed: 17876005]

39. Hammond J. L., Koontz D. L., Bazmi H. Z., Beadle J. R., Hostetler S. E., Kini G. D., Aldern K. A., Richman D. D., Hostetler K. Y., Mellors J. W. (2001) Alkylglycerol prodrugs of phosphonoformate are potent *in vitro* inhibitors of nucleoside-resistant human immunodeficiency virus type 1 and select for resistance mutations that suppress zidovudine resistance. Antimicrob. Agents Chemother. 45, 1621–1628 [PMCID: PMC90523] [PubMed: 11353603]

40. Mellors J. W., Bazmi H. Z., Schinazi R. F., Roy B. M., Hsiou Y., Arnold E., Weir J., Mayers D. L. (1995) Novel mutations in reverse transcriptase of human immunodeficiency virus type 1 reduce susceptibility to foscarnet in laboratory and clinical isolates. Antimicrob. Agents Chemother. 39, 1087–1092 [PMCID: PMC162688] [PubMed: 7542860]

41. Meyer P. R., Lennerstrand J., Matsuura S. E., Larder B. A., Scott W. A. (2003) Effects of dipeptide insertions between codons 69 and 70 of human immunodeficiency virus type 1 reverse transcriptase on primer unblocking, deoxynucleoside triphosphate inhibition, and DNA chain elongation. J. Virol. 77, 3871–3877 [PMCID: PMC149510] [PubMed: 12610164]

42. Tachedjian G., Hooker D. J., Gurusinghe A. D., Bazmi H., Deacon N. J., Mellors J., Birch C., Mills J. (1995) Characterisation of foscarnet-resistant strains of human immunodeficiency virus type 1. Virology 212, 58–68 [PubMed: 7545854]

43. Cases-Gonzalez C. E., Gutierrez-Rivas M., Ménendez-Arias L. (2000) Coupling ribose selection to fidelity of DNA synthesis. The role of Tyr-115 of human immunodeficiency virus type 1 reverse transcriptase. J. Biol. Chem. 275, 19759–19767 [PubMed: 10748215]

44. Gao G., Orlova M., Georgiadis M. M., Hendrickson W. A., Goff S. P. (1997) Conferring RNA polymerase activity to a DNA polymerase: a single residue in reverse transcriptase controls substrate selection. Proc. Natl. Acad. Sci. U.S.A. 94, 407–411 [PMCID: PMC19524] [PubMed: 9012795]

45. Auger A., Beilhartz G. L., Zhu S., Cauchon E., Falgueyret J. P., Grobler J. A., Ehteshami M., Götte M., Melnyk R. A. (2011) Impact of primer-induced conformational dynamics of HIV-1 reverse transcriptase on polymerase translocation and inhibition. J. Biol. Chem. 286, 29575–29583 [PMCID: PMC3190998] [PubMed: 21737446]

46. Sarafianos S. G., Das K., Ding J., Boyer P. L., Hughes S. H., Arnold E. (1999) Touching the heart of HIV-1 drug resistance: the fingers close down on the dNTP at the polymerase active site. Chem. Biol. 6, R137–R146 [PubMed: 10322129]

47. Zahn K. E., Tchesnokov E. P., Götte M., Doublié S. (2011) Phosphonoformic acid inhibits viral replication by trapping the closed form of the DNA polymerase. J. Biol. Chem. 286, 25246–25255 [PMCID: PMC3137095] [PubMed: 21566148]

48. Scarth B., McCormick S., Götte M. (2011) Effects of mutations F61A and A62V in the fingers subdomain of HIV-1 reverse transcriptase on the translocational equilibrium. J. Mol. Biol. 405, 349–360 [PubMed: 21056575]

Figures and Tables

FIGURE 1.

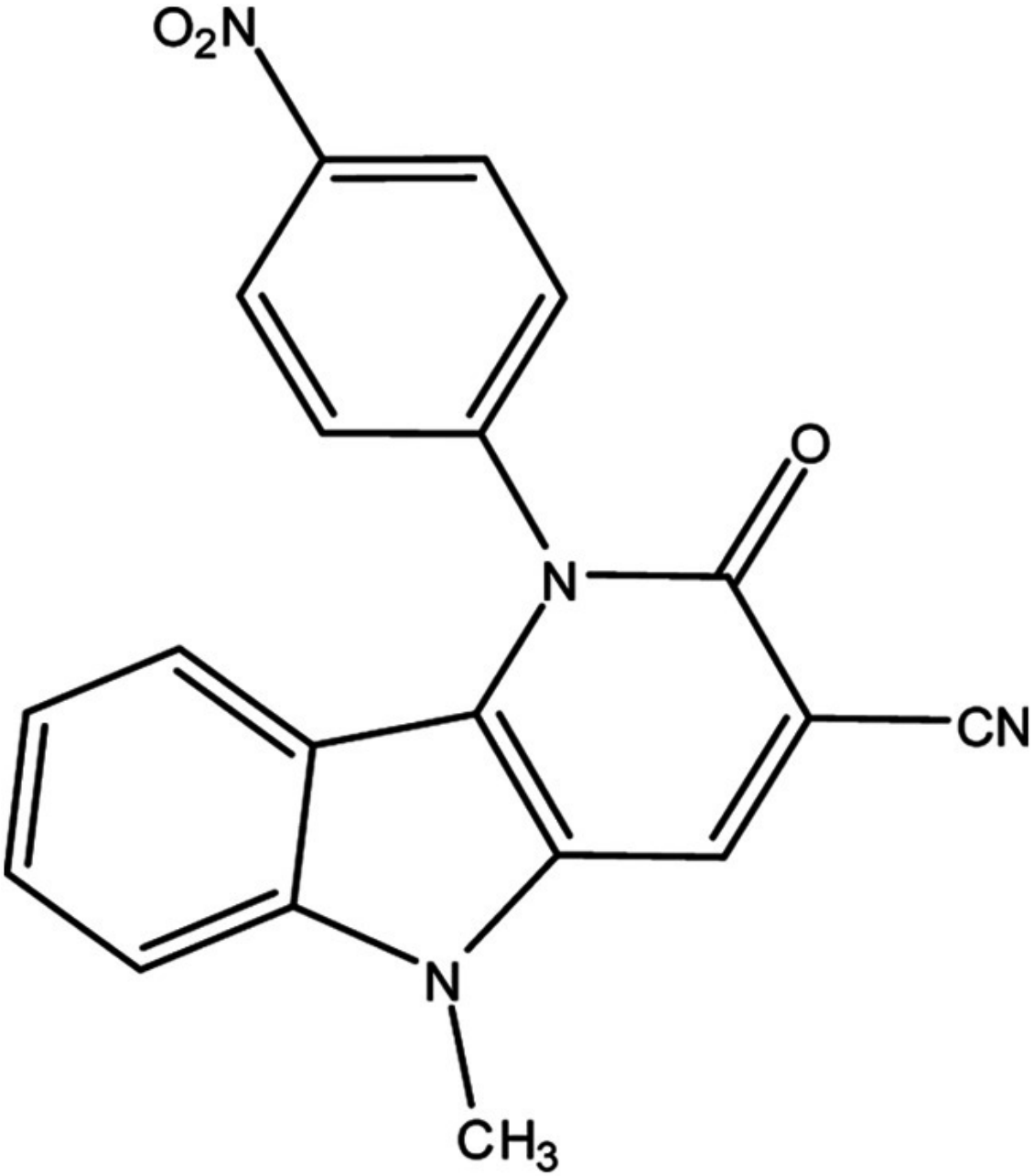

Chemical structure of INDOPY-1. 5-Methyl-1-(4-nitrophenyl)-2-oxo-2,5-dihydro-1*H*-pyrido[3,2-b]indole-3-carbonitrile.

FIGURE 2.

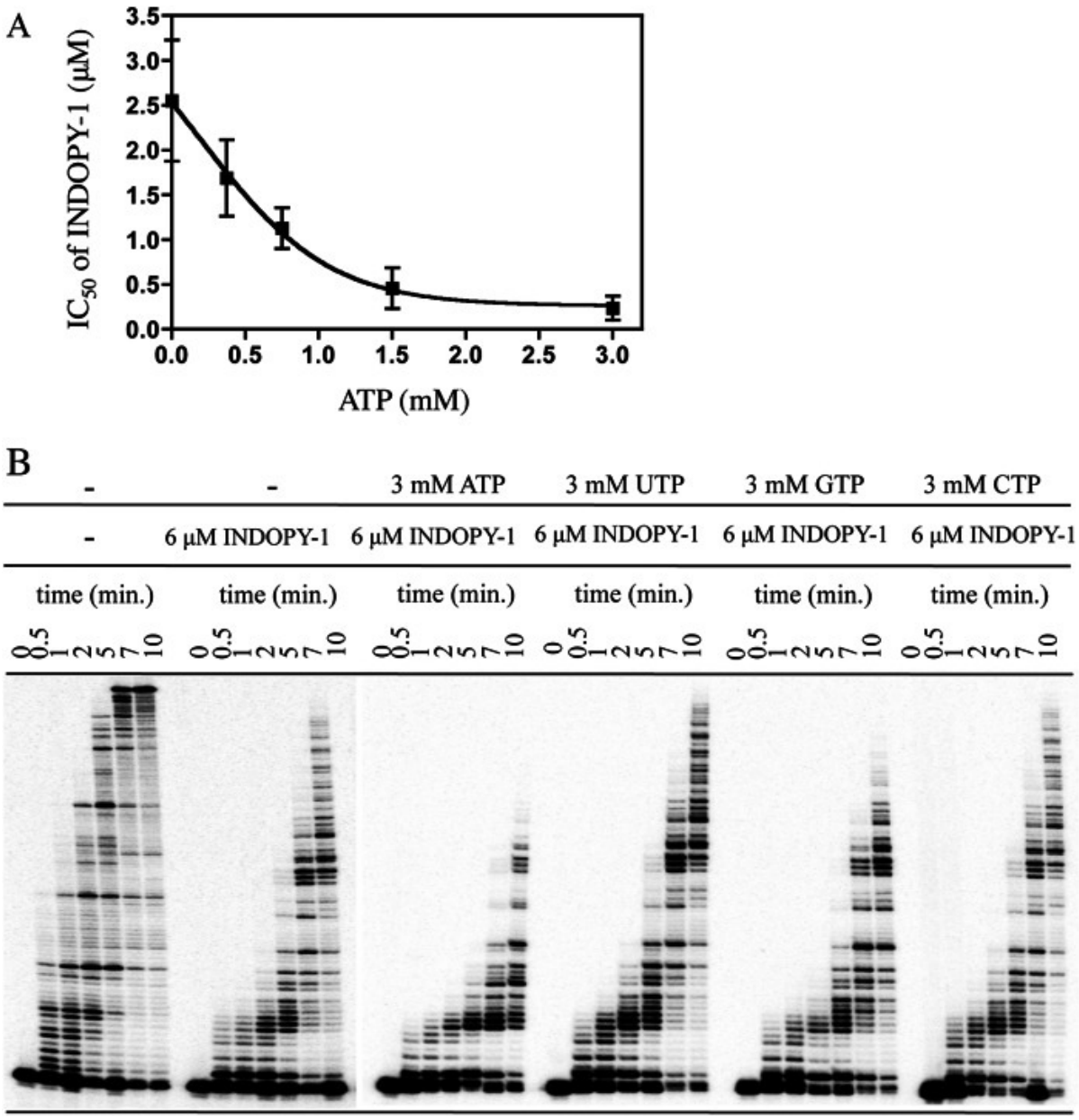

Effect of ATP on INDOPY-1-mediated inhibition of RT. *A,* single nucleotide incorporation was monitored with increasing concentrations of INDOPY-1 in the presence of different ATP levels. Changes in IC_{50} values for INDOPY-1 as a function of ATP concentration are shown in the *graph* ($n = 3$). *B,* multiple nucleotide incorporation was monitored over time on a heteropolymeric RNA template. The assay was repeated in the presence of 10 μM dNTP mix, 6 μM INDOPY-1, as well as 3 mM ATP, UTP, GTP, or CTP. Reduction in full-length product formation is indicative of inhibition.

FIGURE 3.

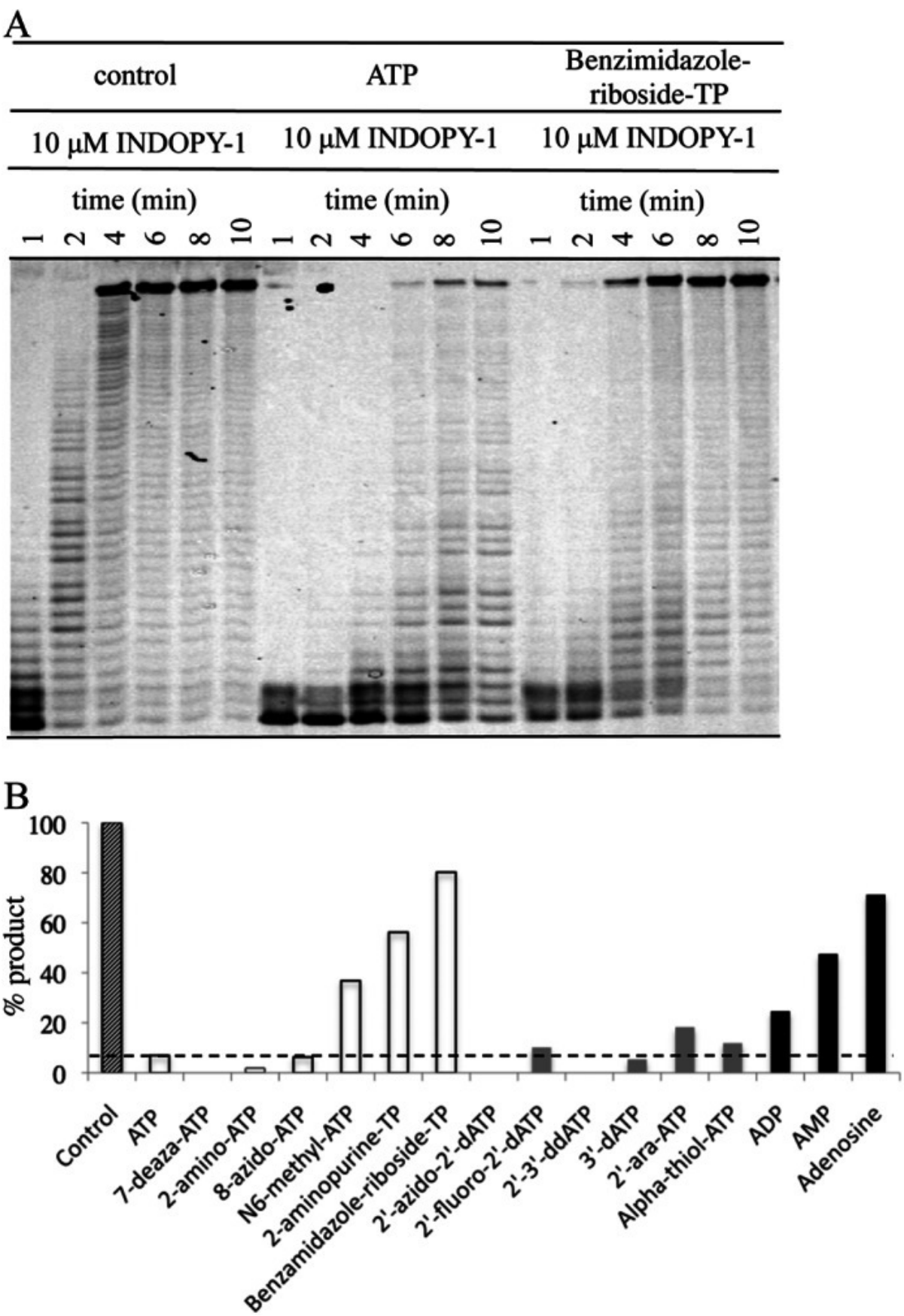

Effect of ATP derivative compounds on INDOPY-1-mediated inhibition of RT. *A,* multiple nucleotide incorporation was monitored over time on a homopolymeric template. DNA synthesis inhibition was monitored in the presence of 10 μM INDOPY-1 alone or with 1 mM ATP or benzimidazole-riboside-TP. *B,* time course assays were repeated for a total of 13 ATP derivatives (chemical structures are provided in supplemental Fig. 1). Amount of DNA product formed at 10 min in the presence of 1 mM ATP derivative and 10 μM INDOPY-1 was quantified and normalized to the amount of DNA product formed at 10 min in the presence of INDOPY-1 alone. *Control bar* represents normalized product formed in the presence of

10 μM INDOPY-1. *Clear bars* represent ATP derivatives with modifications to the base moiety. *Gray bars* represent ATP derivatives with modified sugar moieties, and *black bars* represent ATP derivatives with modified phosphate moieties. Most ATP derivatives were tested in two to three separate experiments.

FIGURE 4.

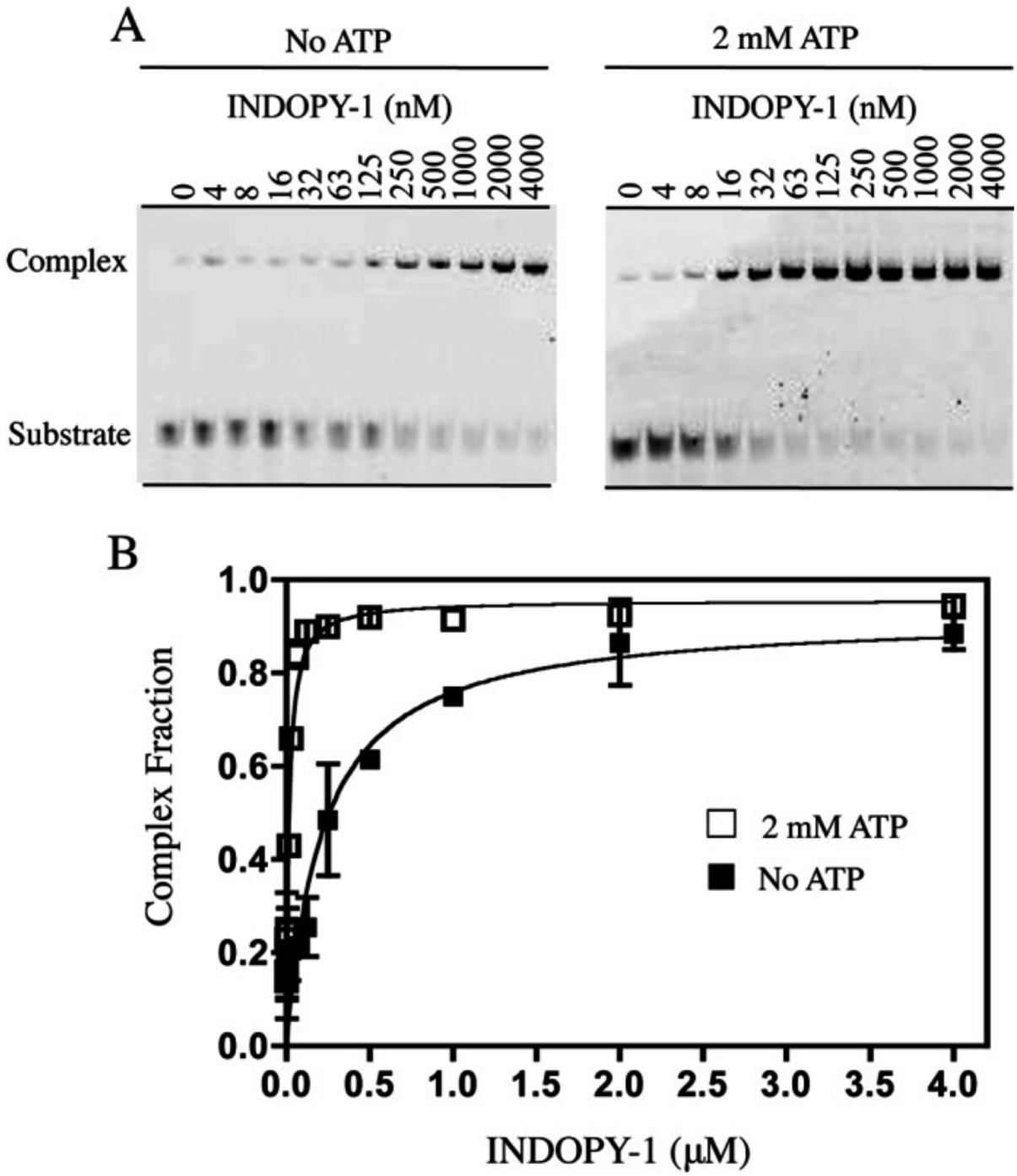

Effect of ATP on stabilization of RT·DNA·DNA· INDOPY-1 complex. *A,* band shift experiment was performed on a DNA·DNA substrate. Conditions were optimized for an unstable binary complex (*lane 0*). As INDOPY-1 concentrations increase, a stable ternary complex is formed, as indicated by the observed shift. The band shift experiment was repeated in the presence of 2 mM ATP. The absence of a significant amount of complex formed in the *0 lane* indicates that in the absence of INDOPY-1 ATP does not stabilize the complex. *B,* amount of complex formed was plotted as a function of INDOPY-1 concentration. Apparent K_d value for INDOPY-1 is 216.5 nM in the absence of ATP and 15.4 nM with ATP.

TABLE 1

MT-2 cell-based EC_{50} values for INDOPY-1

Virus	AZT[a]		INDOPY-1		PFA	
	EC_{50}[b]	FC[c]	EC_{50}	FC	EC_{50}	FC
	μ*M*		μ*M*		μ*M*	
WT	32.6 ± 10.1		54.5 ± 4.7		17.6 ± 7.4	
TAM1	180.6 ± 62.9	5.5	110.9 ± 8.3	2.0	7.9 ± 4.5	0.5
TAM2	130.9 ± 39.7	4.0	262.3 ± 76.7	4.8	10.5 ± 0.1	0.6
Remodeled TAMs	36.0 ± 20.6	1.1	9.4 ± 2.0	0.2	112.3 ± 7.8	6.4

[a] Reported values are based on three separate experiments.

[b] Half-maximal effective concentration (EC_{50}) refers to the inhibitor concentration at which virus replication is reduced by 50% in cell culture assays.

[c] Fold-change (FC) values were obtained by dividing the EC_{50} value of each inhibitor for mutant RT with the corresponding EC_{50} value for WT RT.

FIGURE 5.

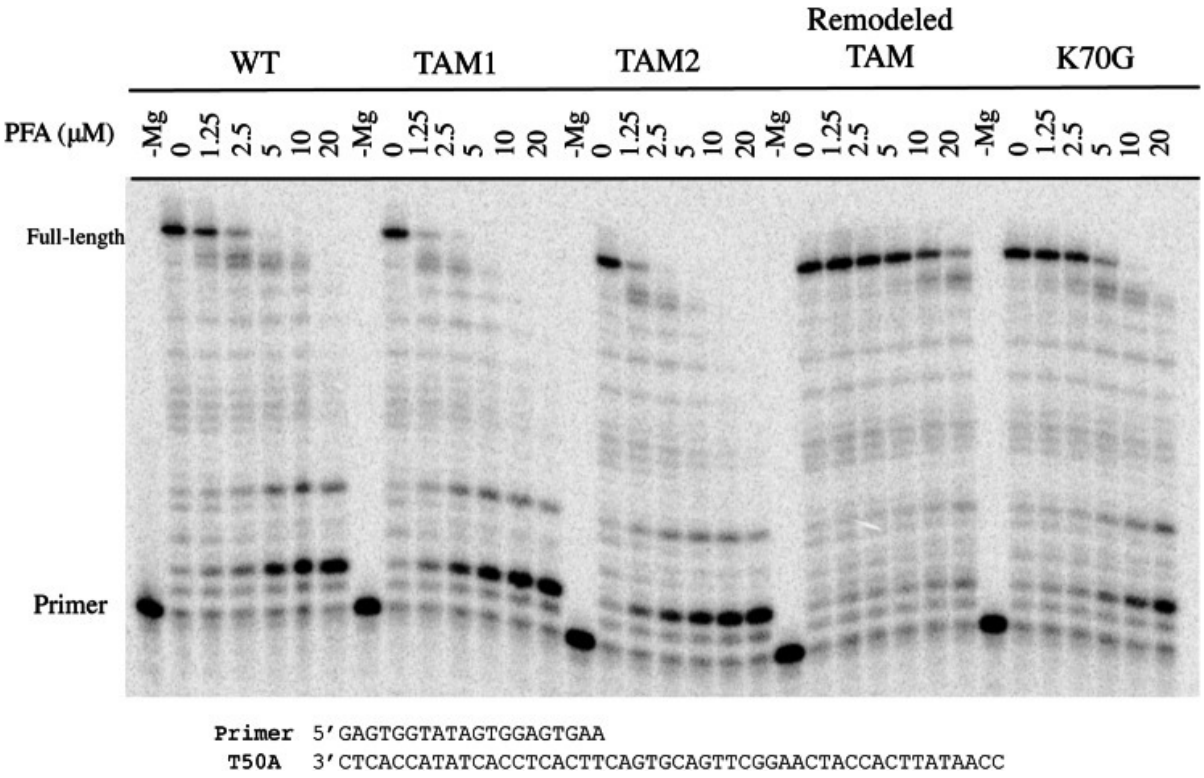

DNA synthesis inhibition by PFA. RT mutants were evaluated for sensitivity to PFA. Each RT mutant was incubated with 1 μM dNTP mix and increasing concentrations of PFA for 10 min at 37 °C. Full-length DNA synthesis was visualized on 12% denaturing polyacrylamide gels. In the absence of magnesium, no polymerization is observed in control lanes.

FIGURE 6.

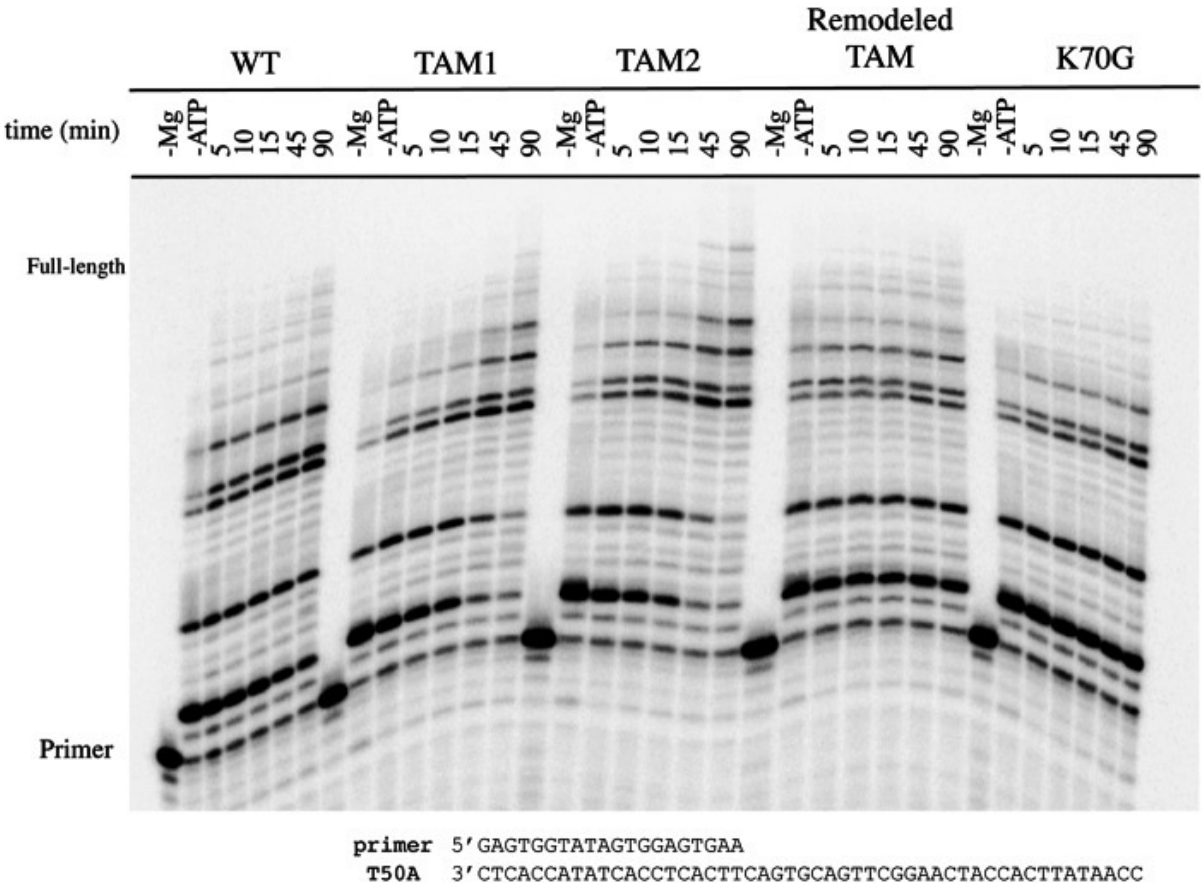

ATP-mediated excision of AZT-MP and rescue of DNA synthesis. DNA·DNA primer·template substrate was incubated with an excess of RT (WT or mutant) and 10 μM AZP-TP in the presence of 0.5 μM dNTPs and 3.5 mM ATP. DNA synthesis and rescue was initiated with the addition of $MgCl_2$ and monitored at various time points up to 90 min. In the absence of magnesium, no polymerization is observed in control lanes.

TABLE 2

***In vitro* IC_{50} values for INDOPY-1 in the presence of increasing ATP**

ATP	IC_{50} [a,b]		
	WT	Remodeled TAMs	FC [c]
mM		*nM*	
0	76.3 ± 28.3	52.0 ± 24.3	0.7
0.1	56.7 ± 30.6	22.0 ± 23.3	0.4
0.3	26.3 ± 12.9	3.4 ± 0.8	0.1
1	10.7 ± 7.4	3.6 ± 2.4	0.3

[a] Reported values are based on three separate experiments.

[b] *In vitro* half-maximal inhibitory concentration (IC_{50}) values were measured using a Quench FRET assay. Because of the experimental setup, namely reduced RT concentrations, the IC_{50} values reported here appear lower than ones reported in Fig. 2*A*.

[c] Fold-change (FC) values were obtained by dividing the IC_{50} value of INDOPY-1 for remodeled TAMs enzyme with that of WT RT for each corresponding ATP concentration.

FIGURE 7.

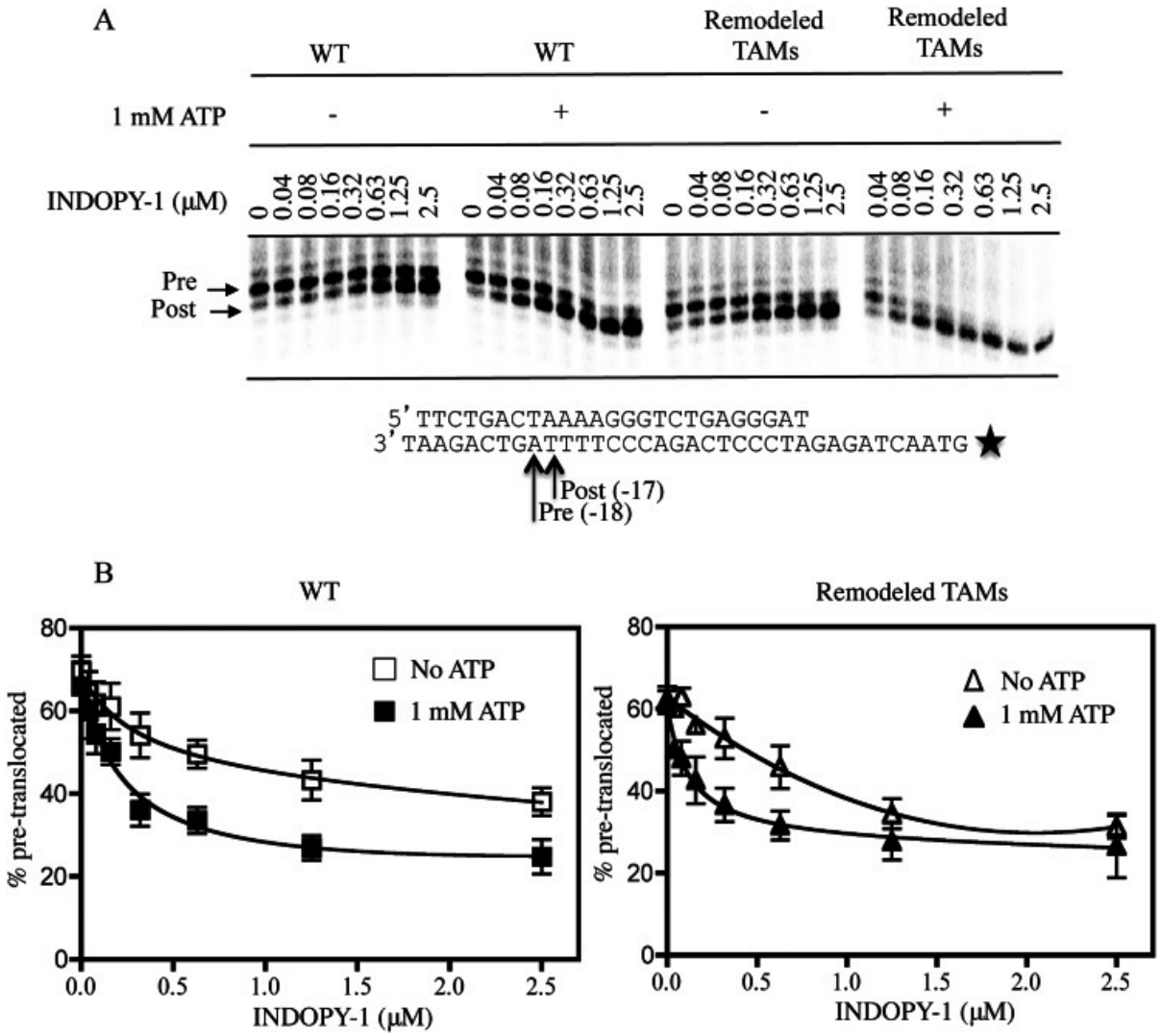

Effect of INDOPY-1 and ATP on enzyme translocation. *A,* 5′-labeled nucleic acid substrate was incubated with an excess of enzyme in the presence of increasing concentrations of INDOPY-1. In the absence of INDOPY-1, the complex shows a bias toward pre-translocation (*lanes 0*). The DNA template was subsequently cleaved with the addition of Fe^{2+} in the presence or absence of 1 mM ATP. The site of DNA cleavage is indicated on the template sequence with *arrows. B,* amount of enzyme in the pre-translocated state was plotted as function of INDOPY-1 concentration.

FIGURE 8.

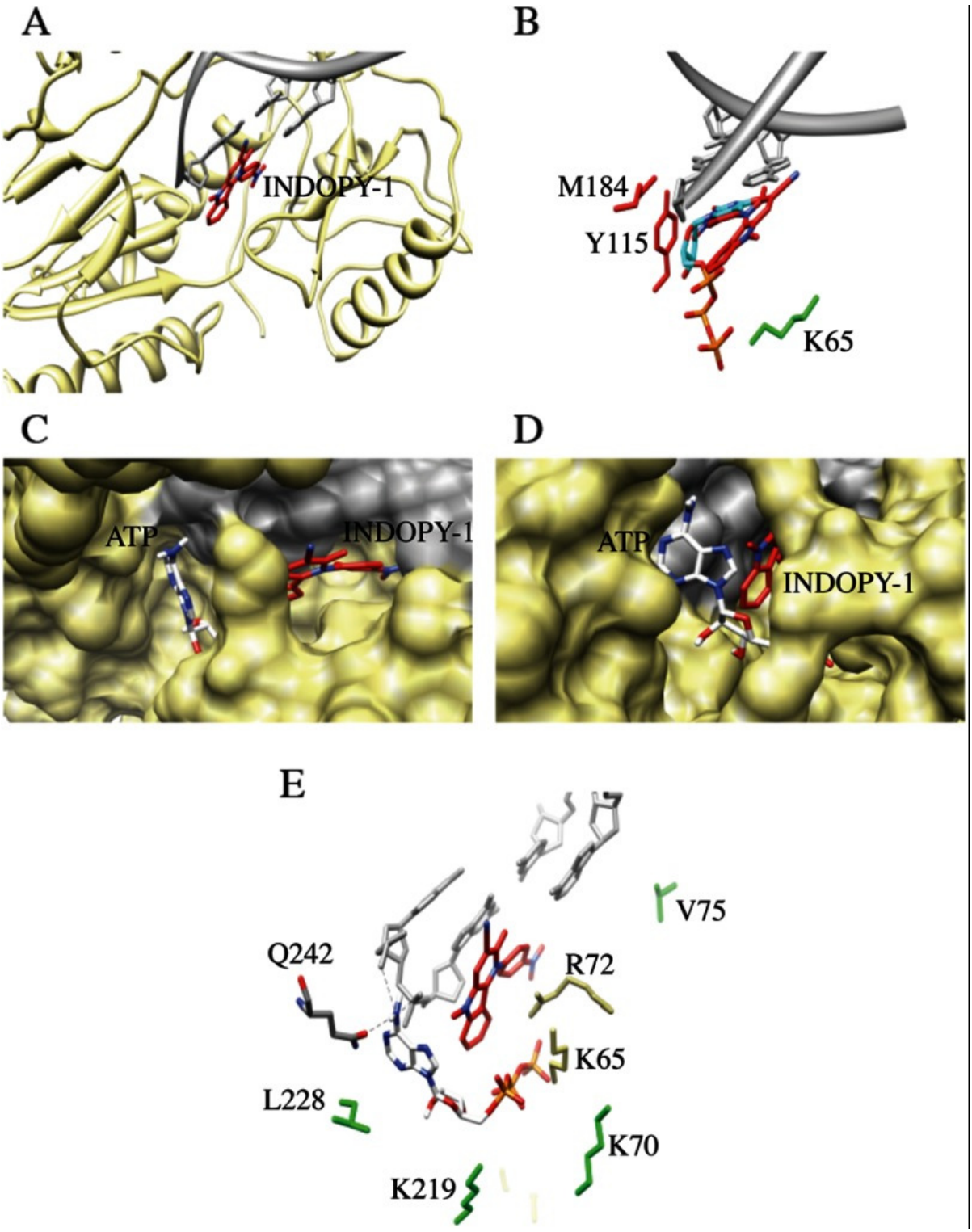

***In silico* modeling of INDOPY-1 and ATP at the polymerase active site.** *A,* INDOPY-1 is colored in *red*; HIV-1 RT is colored in *yellow*, and the DNA hybrid is colored in *gray. B,* position of dTTP (*cyan*) from the 1RTD crystal structure was overlaid with the docking pose of INDOPY-1 (*red*). Shown in *red* are the residues associated with INDOPY-1 resistance (Tyr-115 and Met-184). *C,* ATP was docked to the model containing INDOPY-1. The top view of the surface map of HIV-1 RT is shown with focus on the cavity to which ATP (*white*) binds when INDOPY-1 (*red*) is located at the nucleotide-binding site. *D,* side view of the surface map of HIV-1 RT, highlighting the effect of ATP that prevents INDOPY-1 from dissociating from the RT active site. *E, dashed lines* are shown indicating putative interactions between the critical amino group of adenine base of ATP, the protein and the nucleic acid substrate; the phosphate backbone for the ultimate and penultimate positions in the primer, as well as the terminal amide of the Gln-242 side chain, are located within 5 Å of the amino group. Residues that result in hypersusceptibility to INDOPY-1 are shown in *green*.

and Molecular Biology